ELSEVIER

SCIENCE DIRECT®

PHYSICS LETTERS B

Physics Letters B 560 (2003) 75–86

www.elsevier.com/locate/npe

How two neutrino superbeam experiments do better than one

V. Barger [a], D. Marfatia [b], K. Whisnant [c]

[a] *Department of Physics, University of Wisconsin, Madison, WI 53706, USA*
[b] *Department of Physics, Boston University, Boston, MA 02215, USA*
[c] *Department of Physics and Astronomy, Iowa State University, Ames, IA 50011, USA*

Received 21 November 2002; received in revised form 3 March 2003; accepted 4 March 2003

Editor: M. Cvetič

Abstract

We examine the use of two superbeam neutrino oscillation experiments with baselines $\lesssim 1000$ km to resolve parameter degeneracies inherent in the three-neutrino analysis of such experiments. We find that with appropriate choices of neutrino energies and baselines two experiments with different baselines can provide a much better determination of the neutrino mass ordering than a single experiment alone. Two baselines are especially beneficial when the mass scale for solar neutrino oscillations $\delta m^2_{\rm sol}$ is $\gtrsim 5\times 10^{-5}$ eV^2. We also examine CP violation sensitivity and the resolution of other parameter degeneracies. We find that the combined data of superbeam experiments with baselines of 295 and 900 km can provide sensitivity to both the neutrino mass ordering and CP violation for $\sin^2 2\theta_{13}$ down to 0.03 for $|\delta m^2_{\rm atm}| \simeq 3\times 10^{-3}$ eV^2. It would be advantageous to have a 10% determination of $|\delta m^2_{\rm atm}|$ before the beam energies and baselines are finalized, although if $|\delta m^2_{\rm atm}|$ is not that well known, the neutrino energies and baselines can be chosen to give fairly good sensitivity for a range of $|\delta m^2_{\rm atm}|$.

1. Introduction

Atmospheric neutrino data from Super-Kamiokande provides strong evidence that ν_μ's created in the atmosphere oscillate to ν_τ with mass-squared difference $|\delta m^2_{\rm atm}| \sim 3\times 10^{-3}$ eV^2 and almost maximal amplitude [1]. Furthermore, the recent solar neutrino data from the Sudbury Neutrino Observatory (SNO) establishes that electron neutrinos change flavor as they travel from the Sun to the Earth: the neutral-current measurement is consistent with the solar neutrino flux predicted in the Standard Solar Model [2], while the charged-current measurement shows a depletion of the electron neutrino component relative to the total flux [3]. Global fits to solar neutrino data give a strong preference for the Large Mixing Angle (LMA) solution to the solar neutrino puzzle, with $\delta m^2_{\rm sol} \sim 5\times 10^{-5}$ eV^2 and amplitude close to 0.8 [3,4].

The combined atmospheric and solar data may be explained by oscillations of three neutrinos, that are described by two mass-squared differences, three mixing angles and a CP violating phase. The atmospheric and solar data roughly determine $\delta m^2_{\rm atm}$, $\delta m^2_{\rm sol}$ and the corresponding mixing angles. The LMA solar solution will be tested decisively (and $\delta m^2_{\rm sol}$ measured accurately) by the KamLAND reactor neutrino experiment [5,6]. More precise measurements of the other

E-mail address: whisnant@iastate.edu (K. Whisnant).

0370-2693
doi:10.1016/S0370-2693(03)00334-4

oscillation parameters may be performed in long-baseline neutrino experiments. The low energy beam at MINOS [7] plus experiments with ICARUS [8] and OPERA [9] will allow an accurate determination of the atmospheric neutrino parameters and may provide the first evidence for oscillations of $\nu_\mu \to \nu_e$ at the atmospheric mass scale [10]. It will take a new generation of long-baseline experiments to further probe $\nu_\mu \to \nu_e$ appearance and to measure the leptonic CP phase. Matter effects are the only means to determine $\mathrm{sgn}(\delta m^2_{\rm atm})$; once $\mathrm{sgn}(\delta m^2_{\rm atm})$ is known, the level of intrinsic CP violation may be measured. Matter effects and intrinsic CP violation both vanish in the limit that the mixing angle responsible for $\nu_\mu \to \nu_e$ oscillations of atmospheric neutrinos is zero.

It is now well known that there are three two-fold parameter degeneracies that can occur in the measurement of the oscillation amplitude for $\nu_\mu \to \nu_e$ appearance, the ordering of the neutrino masses, and the CP phase [11]. With only one ν and one $\bar{\nu}$ measurement, these degeneracies can lead to eight possible solutions for the oscillation parameters; in most cases, CP violating (CPV) and CP conserving (CPC) solutions can equally explain the same data. Studies have been done on how a superbeam [11–16], neutrino factory [16–18], superbeam plus neutrino factory [19], or two superbeams with one at a very long baseline [20,21] could be used to resolve one or more of these ambiguities.

In this Letter we show that by combining the results of two superbeam experiments with different medium baselines, $\lesssim 1000$ km, the ambiguity associated with the sign of $\delta m^2_{\rm atm}$ can be resolved, even when it cannot be resolved by the two experiments taken separately. Furthermore, the ability to determine $\mathrm{sgn}(\delta m^2_{\rm atm})$ from the combined data is found to not be greatly sensitive to the size of $\delta m^2_{\rm sol}$, unlike the situation where data from only a single baseline is used. If both experiments are at or near the peak of the oscillation, a good compromise is obtained between the sensitivities for resolving $\mathrm{sgn}(\delta m^2_{\rm atm})$ and for establishing the existence of CP violation. If $|\delta m^2_{\rm atm}|$ is not known accurately, the neutrino energies and baselines can be chosen to give fairly good sensitivity to the sign of $\delta m^2_{\rm atm}$ and to CP violation for a range of $|\delta m^2_{\rm atm}|$.

The organization of our Letter is as follows. In Section 2 we discuss the parameter degeneracies that can occur in the analysis of long-baseline oscillation data. In Section 3 we analyze how two long-baseline superbeam experiments can break degeneracies, determine the neutrino parameters, and establish the existence of CP violation in the neutrino sector, if it is present. A summary is presented in Section 4.

2. Parameter degeneracies

We work in the three-neutrino scenario using the parametrization for the neutrino mixing matrix of Ref. [11]. If we assume that ν_3 is the neutrino eigenstate that is separated from the other two, then $\delta m^2_{31} = \delta m^2_{\rm atm}$ and the sign of δm^2_{31} can be either positive or negative, corresponding to the mass of ν_3 being either larger or smaller, respectively, than the other two masses. The solar oscillations are regulated by $\delta m^2_{21} = \delta m^2_{\rm sol}$, and thus $|\delta m^2_{21}| \ll |\delta m^2_{31}|$. If we accept the likely conclusion that the solar solution is LMA [3,4], then $\delta m^2_{21} > 0$ and we can restrict θ_{12} to the range $[0, \pi/4]$. It is known from reactor neutrino data that θ_{13} is small, with $\sin^2 2\theta_{13} \leqslant 0.1$ at the 95% C.L. [22]. Thus a set of parameters that unambiguously spans the space is δm^2_{31} (magnitude and sign), δm^2_{21}, $\sin^2 2\theta_{12}$, $\sin\theta_{23}$, and $\sin^2 2\theta_{13}$; only the θ_{23} angle can be below or above $\pi/4$.

For the oscillation probabilities for $\nu_\mu \to \nu_e$ and $\bar{\nu}_\mu \to \bar{\nu}_e$ we use approximate expressions given in Ref. [11], in which the probabilities are expanded in terms of the small parameters θ_{13} and δm^2_{21} [23, 24], which reproduces well the exact oscillation probabilities for $E_\nu \gtrsim 0.5$ GeV, $\theta_{13} \lesssim 9^\circ$, and $L \lesssim 4000$ km [11]. In all of our calculations we use the average electron density along the neutrino path, assuming the preliminary reference Earth model [25]. Our calculational methods are described in Ref. [12].

We expect that $|\delta m^2_{31}|$ and $\sin^2 2\theta_{23}$ will be measured to an accuracy of $\simeq 10\%$ at 3σ from $\nu_\mu \to \nu_\mu$ survival in long-baseline experiments [7–10], while δm^2_{21} will be measured to an accuracy of $\simeq 10\%$ at 2σ and $\sin^2 2\theta_{12}$ will be measured to an accuracy of ± 0.1 at 2σ in experiments with reactor neutrinos [6]. The remaining parameters (θ_{13}, the CP phase δ, and the sign of δm^2_{31}) must be determined from long-baseline appearance experiments, principally using the modes $\nu_\mu \to \nu_e$ and $\bar{\nu}_\mu \to \bar{\nu}_e$ with conventional neutrino beams, or $\nu_e \to \nu_\mu$ and $\bar{\nu}_e \to \bar{\nu}_\mu$ at neutrino factories.

However, there are three parameter degeneracies that can occur in such an analysis: (i) the (δ, θ_{13}) ambiguity [17], (ii) the $\mathrm{sgn}(\delta m^2_{31})$ ambiguity [13], and (iii) the $(\theta_{23}, \pi/2 - \theta_{23})$ ambiguity [11,26] (see Ref. [11] for a complete discussion of these three parameter degeneracies). In each degeneracy, two different sets of values for δ and θ_{13} can give the same measured rates for both ν and $\bar{\nu}$ appearance and disappearance. For each type of degeneracy the values of θ_{13} for the two equivalent solutions can be quite different, and the two values of δ may have different CP properties, e.g., one can be CP conserving and the other CP violating.

A judicious choice of L and E_ν can reduce the impact of the degeneracies. For example, if L/E_ν is chosen such that $\Delta \equiv |\delta m^2_{31}| L/(4E_\nu) = \pi/2$ (the peak of the oscillation in vacuum), then the $\cos\delta$ terms in the average appearance probabilities vanish, even after matter effects are included [11]. Then since it is $\sin\delta$ that is being measured, the (δ, θ_{13}) ambiguity is reduced to a simple $(\delta, \pi - \delta)$ ambiguity, CPV solutions are no longer mixed with CPC solutions, and θ_{13} is, in principle, determined (for a given $\mathrm{sgn}(\delta m^2_{31})$ and θ_{23}). If L is chosen to be long enough ($\gtrsim 1000$ km), then the predictions for $\delta m^2_{31} > 0$ and $\delta m^2_{31} < 0$ no longer overlap if $\theta_{13} \gtrsim$ a few degrees, and the $\mathrm{sgn}(\delta m^2_{31})$ ambiguity is removed; our previous studies indicated that for $\delta m^2_{21} = 5 \times 10^{-5}$ eV^2 this happens at $L \gtrsim 1300$ km if $\sin^2 2\theta_{13} > 0.01$ [11] (before experimental uncertainties are considered). However, the persistence of the $\mathrm{sgn}(\delta m^2_{31})$ ambiguity is highly dependent on the size of the solar oscillation mass scale, because large values of δm^2_{21} cause the predictions for $\delta m^2_{31} > 0$ and $\delta m^2_{31} < 0$ to overlap much more severely than when δm^2_{21} is smaller. Also, existing neutrino baselines are no longer than 735 km. In this Letter we explore the possibility that two experiments with medium baselines ($\lesssim 1000$ km) can determine $\mathrm{sgn}(\delta m^2_{31})$, even when data from one of the baselines alone cannot. We then address the sensitivity for establishing CP violation.

3. Joint analysis of two superbeam experiments

3.1. Description of the experiments and method

For our analysis we take one baseline to be 295 km, the distance for the proposed experiment from the Japan Hadron facility (JHF) to the Super-Kamiokande detector at Kamioka. For the differential rates (flux times cross section per kiloton-year vs. neutrino energy) of this experiment we use their 2° off-axis beam with average neutrino energy of 0.7 GeV [27]. For the second experiment we assume an off-axis beam in which the beam axis points at a site 735 km from the source (appropriate for a beamline from NuMI at Fermilab to Soudan, or from CERN to Gran Sasso). For the off-axis beam of the NuMI experiment we use the results presented in Ref. [28], which provides differential rates for 39 different off-axis angles ranging from 0.32° to 1.76°. We calculate the total number of events by integrating the differential event rate times oscillation probability for each experiment, using the energy ranges 0.11–10.0 GeV for the JHF spectra and 0.2–20 GeV for NuMI spectra.

Using the off-axis components of the beam has the advantage of a lower background [15,29,30] due to reduced ν_e contamination and a smaller high-energy tail. Off-axis beams also offer flexibility in the choice of L and E_ν. For example, for a beam nominally aimed at a ground-level site a distance L_0 from the source, the distance to a ground-level detector with off-axis angle θ_{OA} can lie anywhere in the range

$$2R_e \sin(\theta - \theta_{\mathrm{OA}}) \leqslant L \leqslant 2R_e \sin(\theta + \theta_{\mathrm{OA}}), \tag{1}$$

where $\sin\theta = L_0/(2R_e)$, and $R_e = 6371$ km is the radius of the Earth. Then for $L_0^2 \ll R_e^2$ the possible range of distances for an off-axis detector at approximately ground level is

$$L_0 - 2R_e\theta_{\mathrm{OA}} \lesssim L \lesssim L_0 + 2R_e\theta_{\mathrm{OA}}. \tag{2}$$

The neutrino energy and neutrino flux Φ_ν decrease with increasing off-axis angle as

$$E_\nu = \frac{0.43E_\pi}{1 + \gamma^2\theta^2_{\mathrm{OA}}}, \qquad \Phi_\nu \propto \frac{E_\nu^2}{L^2}, \tag{3}$$

where $\gamma = E_\pi/m_\pi$ is boost factor of the decaying pion. Thus a wide range of L and E_ν can be achieved with a single fixed beam, although the event rate will drop with increasing off-axis angle because the flux decreases and the neutrino cross section is smaller at smaller E_ν (thereby putting a limit on the usable range of L and E_ν).

For the first experiment at $L_1 = 295$ km, we assume that the neutrino spectrum is chosen so that the

$\cos\delta$ terms in the ν and $\bar{\nu}$ oscillation probabilities vanish (after averaging over the neutrino spectrum), using the best existing experimental value for δm^2_{31}. The JHF 2° off-axis beam [31] satisfies this condition for $\delta m^2_{31} = 3 \times 10^{-3}$ eV^2. This spectrum choice reduces the (δ, θ_{13}) ambiguity to a simple $(\delta, \pi - \delta)$ ambiguity, as described in Section 2. For the second experiment we allow L_2 and $\theta_{\rm OA}$ to vary within the restrictions of Eq. (2). This flexibility can be fully utilized if a deep underground site is not required; the short duration of the beam operation (an 8.6 μs pulse with a 1.9 s cycle time [32]) may enable a sufficient reduction in the cosmic ray neutrino background. We assume that the proton drivers at the neutrino sources have been upgraded from their initial designs (from 0.8 to 4.0 MW for JHF [31] and from 0.4 to 1.6 MW for FNAL [33]), so that they are both true neutrino superbeams. We assume two years running with neutrinos and six years with antineutrinos at JHF, and two years with neutrinos and five years with antineutrinos at FNAL; these running times give approximately equivalent numbers of charged-current events for neutrinos and antineutrinos at the two facilities, in the absence of oscillations. For detectors, we assume a 22.5 kt detector in the JHF beam (such as the current Super-Kamiokande detector) and a 20 kt detector in the FNAL beam (which was proposed in Ref. [15]). Larger detectors such as Hyper-Kamiokande or UNO would allow shorter beam exposures or higher precision studies. In all of our calculations, we assume $|\delta m^2_{31}| = 3 \times 10^{-3}$ eV^2, $\theta_{23} = \pi/4$, $\delta m^2_{21} = 5 \times 10^{-5}$ eV^2, and $\sin^2 2\theta_{12} = 0.8$, unless noted otherwise.

We first consider the minimum value of $\sin^2 2\theta_{13}$ for which the signal in the neutrino appearance channel can be seen above background at the 3σ level (the discovery reach), varying over a range of allowed values for $\theta_{\rm OA}$ and L_2 in the second experiment. The discovery reach depends on the value of δ and the sign of δm^2_{31}; the best (when $\delta m^2_{31} > 0$) and worst (when $\delta m^2_{31} < 0$) cases in the ν channel (after varying over δ) are shown in Fig. 1. In the $\bar{\nu}$ channel, the best case occurs for $\delta m^2_{31} < 0$ and the worst for $\delta m^2_{31} > 0$. In our calculations we assume a background that is 0.5% of the unoscillated charged-current rate (see Ref. [15]), and that the systematic error is 5% of the background. The statistical uncertainty of the signal plus background events and the assumed systematic uncertainty are added in quadrature. However, we note that our general conclusions are not significantly affected by reasonable changes in these experimental uncertainty assumptions. Detector positions where there are no

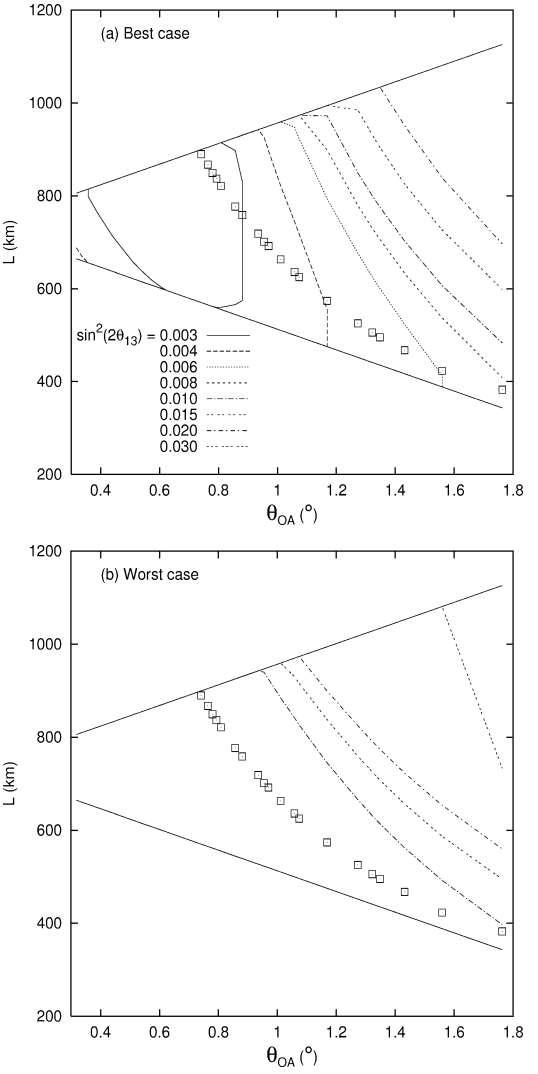

Fig. 1. Contours of (a) best-case (when $\delta m^2_{31} > 0$), and (b) worst-case (when $\delta m^2_{31} < 0$), $\sin^2 2\theta_{13}$ 3σ discovery reach in the $(\theta_{\rm OA}, L_2)$ plane, for the ν channel at NuMI, where $\theta_{\rm OA}$ is the off-axis angle and L_2 is the baseline of the NuMI detector. For the other neutrino parameters we assume $|\delta m^2_{31}| = 3 \times 10^{-3}$ eV^2, $\theta_{23} = \pi/4$, $\delta m^2_{21} = 5 \times 10^{-5}$ eV^2, and $\sin^2 2\theta_{12} = 0.8$. The boxes indicate detector positions for which the $\cos\delta$ terms in the average oscillation probabilities vanish. For the $\bar{\nu}$ channel the results are similar, except that the best case occurs for $\delta m^2_{31} < 0$ and the worst case for $\delta m^2_{31} > 0$.

Table 1
Number of $\nu_\mu \to \nu_\mu$ survival, and $\nu_\mu \to \nu_e$ and $\bar{\nu}_\mu \to \bar{\nu}_e$ signal and background events for the JHF and NuMI experiments, shown for several values of $\sin^2 2\theta_{13}$ and δ. The other oscillation parameters are chosen to be the standard values described in the text. The NuMI detector is placed at $L = 890$ km and $\theta_{\rm OA} = 0.74°$

$\sin^2 2\theta_{13}$	δ	JHF			NuMI		
		$\nu_\mu \to \nu_\mu$ survival	$\nu_\mu \to \nu_e$ S/B	$\bar{\nu}_\mu \to \bar{\nu}_e$ S/B	$\nu_\mu \to \nu_\mu$ survival	$\nu_\mu \to \nu_e$ S/B	$\bar{\nu}_\mu \to \bar{\nu}_e$ S/B
0.01	90°	22980	46/115	85/102	14210	43/71	60/71
	270°	22980	103/115	36/102	14210	94/71	21/71
0.03	90°	22980	164/115	216/102	14210	154/71	149/71
	270°	22980	263/115	132/102	14210	243/71	82/71

$\cos\delta$ dependence in the rates are denoted by boxes. The best reach is $\sin^2 2\theta_{13} \simeq 0.003$, which occurs for $\theta_{\rm OA} \simeq 0.5$–$0.9°$. In the worst case scenario the reach degrades to $\sin^2 2\theta_{13} \simeq 0.01$. Table 1 shows the number of $\nu_\mu \to \nu_\mu$ survival, and $\nu_\mu \to \nu_e$ and $\bar{\nu}_\mu \to \bar{\nu}_e$ signal and background events for several values of $\sin^2 2\theta_{13}$ and δ when $L = 890$ km and $\theta_{\rm OA} = 0.74°$ for the NuMI detector.

The measurement of P and $\overline{P}$ at L_1 allows a determination of $\sin^2 2\theta_{13}$ and $\sin\delta$, modulo the possible uncertainty caused by the sign of δm^2_{31}, assuming for the moment that $\theta_{23} = \pi/4$, so there is no $(\theta_{23}, \pi/2 - \theta_{23})$ ambiguity. The question we next consider is whether an additional measurement of P and $\overline{P}$ at L_2 can determine $\mathrm{sgn}(\delta m^2_{31})$, measure CP violation, and distinguish δ from $\pi - \delta$. We define the χ^2 of neutrino parameters (δ', θ'_{13}) relative to the parameters (δ, θ_{13}) as

$$\chi^2 = \sum_i \frac{(N_i - N'_i)^2}{(\delta N_i)^2}, \tag{4}$$

where N_i and N'_i are the event rates for the parameters (δ, θ_{13}) and (δ', θ'_{13}), respectively, δN_i is the uncertainty in N_i, and i is summed over the measurements being used in the analysis (ν and $\bar{\nu}$ at L_1 and ν and $\bar{\nu}$ at L_2). For δN_i we assume that the statistical error for the signal plus background can be added in quadrature with the systematic error. For a two-parameter system (δ and θ_{13} unknown), two sets of parameters can be resolved at the 2σ (3σ) level if $\chi^2 > 6.17$ (11.83).

3.2. Determining the sign of δm^2_{31}

To determine if measurements at L_1 and L_2 can distinguish one set of oscillation parameters with one sign of δm^2_{31} from all other possible sets of oscillation parameters with the opposite sign of δm^2_{31}, we sample the (δ, θ_{13}) space for the opposite $\mathrm{sgn}(\delta m^2_{31})$ using a fine grid with 1° spacing in δ and approximately 2% increments in $\sin^2 2\theta_{13}$. If the χ^2 between the original set of oscillation parameters and all of those with the opposite $\mathrm{sgn}(\delta m^2_{31})$ is greater than 6.17 (11.83), then $\mathrm{sgn}(\delta m^2_{31})$ is distinguished at the 2σ (3σ) level for that parameter set.

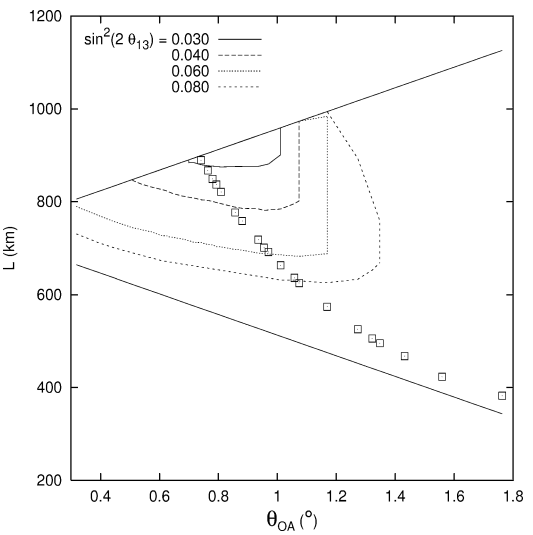

Fig. 2. Contours of $\sin^2 2\theta_{13}$ reach for resolving the sign of δm^2_{31} at the 3σ level in the $(\theta_{\rm OA}, L_2)$ plane when data from JHF and NuMI are used. The JHF detector is assumed to have baseline $L_1 = 295$ km. Other parameters and notation are the same as in Fig. 1.

Fig. 2 shows contours (in the space of possible L_2 and $\theta_{\rm OA}$ for the second experiment) for the minimum value of $\sin^2 2\theta_{13}$ (the $\sin^2 2\theta_{13}$ reach) for which $\mathrm{sgn}(\delta m^2_{31})$ may be determined at the 3σ level when

Table 2
$\sin^2 2\theta_{13}$ reach for determining the sign of δm^2_{31} at 3σ using ν and $\bar{\nu}$ data from JHF at 295 km and NuMI at L_2, for various detector sizes and proton driver powers. The approximate range of $\theta_{\rm OA}$ that can obtain the reach shown is given in parentheses; $L_2 \sim 900$ km in all cases

JHF	NuMI (20 kt)	
	0.4 MW $\sin^2 2\theta_{13}$ ($\theta_{\rm OA}$)	1.6 MW $\sin^2 2\theta_{13}$ ($\theta_{\rm OA}$)
no JHF data	0.09 (0.7–1.0°)	0.05 (0.8–1.0°)
22.5 kt, 0.8 MW	0.07 (0.8–1.0°)	0.04 (0.9–1.0°)
22.5 kt, 4.0 MW	0.06 (0.7–1.0°)	0.03 (0.7–1.0°)
450 kt, 4.0 MW	0.05 (0.6–1.0°)	0.02 (0.7–0.9°)

ν and $\bar{\nu}$ data from L_1 and L_2 are combined. As in Fig. 1, the boxes indicate the detector positions where the $\cos\delta$ terms in the average probabilities vanish. For the $\delta m^2_{31} > 0$ solution, $\delta = 90°$ is chosen since it has the most serious overlap problem with the $\delta m^2_{31} < 0$ solutions.

The best reach of about $\sin^2 2\theta_{13} \simeq 0.03$ for $\mathrm{sgn}(\delta m^2_{31})$ determination can be realized for $\theta_{\rm OA} \simeq 0.7$–$1.0°$ and L_2 values near the maximum allowed by Eq. (2) ($\simeq$ 875–950 km). Table 2 shows the sensitivity for determining $\mathrm{sgn}(\delta m^2_{31})$ for different combinations of detector size and proton driver power in the two experiments. The table shows that once enough statistics are obtained at JHF (with a 22.5 kt detector and a 4 MW source), combined JHF and NuMI data significantly improve the $\sin^2 2\theta_{13}$ reach for determining $\mathrm{sgn}(\delta m^2_{31})$ at 3σ (by nearly a factor of two compared to data from a 1.6 MW NuMI alone).

The ability to distinguish the sign of δm^2_{31} is greatly affected by the size of the solar mass scale δm^2_{21}, because the predictions for $\delta m^2_{31} > 0$ and $\delta m^2_{31} < 0$ overlap more for larger values of δm^2_{21}. In Fig. 3(a) we show the region in $(\delta, \sin^2 2\theta_{13})$ space for which parameters with $\delta m^2_{31} > 0$ can be distinguished from all parameters with $\delta m^2_{31} < 0$ at the 3σ level for several possible values of δm^2_{21}, using combined data from $L_1 = 295$ km and $L_2 = 890$ km, with $\theta_{\rm OA} = 0.74°$ for the second experiment. With this configuration the $\cos\delta$ terms in the average probabilities vanish for both experiments and nearly maximal reach for distinguishing $\mathrm{sgn}(\delta m^2_{31})$ is achieved. A similar plot using only data at $L_2 = 890$ km and $\theta_{\rm OA} = 0.74°$ is shown in Fig. 3(b). We do not show a corresponding plot for

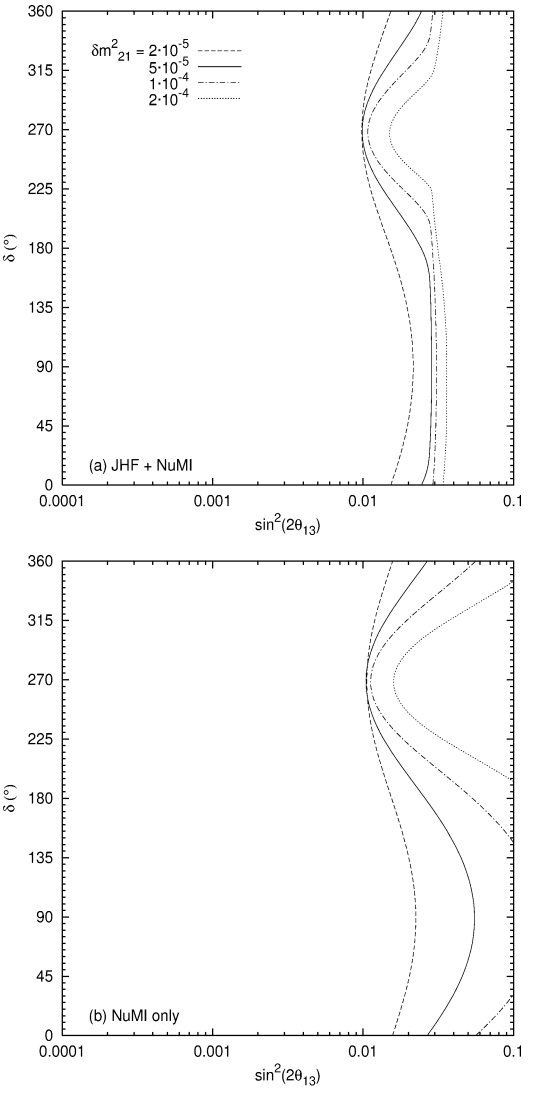

Fig. 3. Minimum value of $\sin^2 2\theta_{13}$ for which $\mathrm{sgn}(\delta m^2_{31})$ may be determined at 3σ, assuming the true solution has $\delta m^2_{31} > 0$, using ν and $\bar{\nu}$ data from (a) JHF with $L_1 = 295$ km and NuMI with $L_2 = 890$ km, and (b) only NuMI with $L_2 = 890$ km, for several values of δm^2_{21} (in eV^2). The off-axis angle for the NuMI detector is $\theta_{\rm OA} = 0.74°$. Other parameters are the same as in Fig. 1. Results for $\delta m^2_{31} < 0$ are approximately given by reflecting the curves about $\delta = 180°$.

$L_1 = 295$ km because the shorter baseline severely inhibits the determination of $\mathrm{sgn}(\delta m^2_{31})$. A comparison of the two figures shows that for $\delta = 270°$ (where the $\delta m^2_{31} > 0$ predictions have the least overlap with any

Table 3
$\sin^2 2\theta_{13}$ reach for determining the sign of δm^2_{31} at 3σ using ν and $\bar{\nu}$ data from JHF at 295 km and NuMI at $L_2 = 890$ km with $\theta_{\rm OA} = 0.74°$, for different combinations of $\mathrm{sgn}(\delta m^2_{31})$ and θ_{23}, where $\sin^2 2\theta_{23} = 0.9$

$\mathrm{sgn}(\delta m^2_{31})$	$\sin^2 2\theta_{13}$ reach for $\mathrm{sgn}(\delta m^2_{31})$	
	$\sin\theta_{23} = 0.585$	$\sin\theta_{23} = 0.811$
+	0.04	0.02
−	0.03	0.03

of those for $\delta m^2_{31} < 0$) the sensitivity to $\mathrm{sgn}(\delta m^2_{31})$ is not significantly improved by adding the data at L_1. However, at $\delta = 90°$ the ability to distinguish $\mathrm{sgn}(\delta m^2_{31})$ is much less affected by the value of δm^2_{21} when the data at L_1 is included. With data only at L_2, $\mathrm{sgn}(\delta m^2_{31})$ can be determined for $\sin^2 2\theta_{13} = 0.1$ when $\delta = 90°$ only for $\delta m^2_{21} \lesssim 8 \times 10^{-5}$ eV^2, while with data at L_1 and L_2 it can be determined for $\sin^2 2\theta_{13}$ as low as 0.04 for δm^2_{21} as high as 2×10^{-4} eV^2. The corresponding results for $\delta m^2_{31} < 0$ are approximately given by reflecting the curves in Fig. 3 about $\delta = 180°$.

We conclude that combining measurements of $\nu_\mu \to \nu_e$ and $\bar{\nu}_\mu \to \bar{\nu}_e$ from two superbeam experiments at different L results in a much more sensitive test of the sign of δm^2_{31} than one experiment alone, especially for larger values of the solar mass scale δm^2_{21}.

The ability to determine $\mathrm{sgn}(\delta m^2_{31})$ is also affected by the value of θ_{23}. We found that the $\sin^2 2\theta_{13}$ reach for determining $\mathrm{sgn}(\delta m^2_{31})$ at 3σ varied from 0.02 to 0.04 for $\sin^2 2\theta_{23} = 0.90$ (compared to 0.03 when $\theta_{23} = \pi/4$), depending on whether δm^2_{31} is positive or negative, and whether $\theta_{23} < \pi/4$ or $\theta_{23} > \pi/4$. The $\mathrm{sgn}(\delta m^2_{31})$ sensitivities for different possibilities are shown in Table 3.

3.3. Establishing the existence of CP violation

An important goal of long-baseline experiments is to determine whether or not CP is violated in the leptonic sector. In order to unambiguously establish the existence of CP violation, one must be able to differentiate between (δ, θ_{13}) and all possible (δ', θ'_{13}), where $\delta' = 0°$ or $180°$ and θ'_{13} can take on any value. For our CP violation analysis we vary $\sin^2 2\theta'_{13}$ in 2% increments, as was done in the previous section when testing the $\mathrm{sgn}(\delta m^2_{13})$ sensitivity.

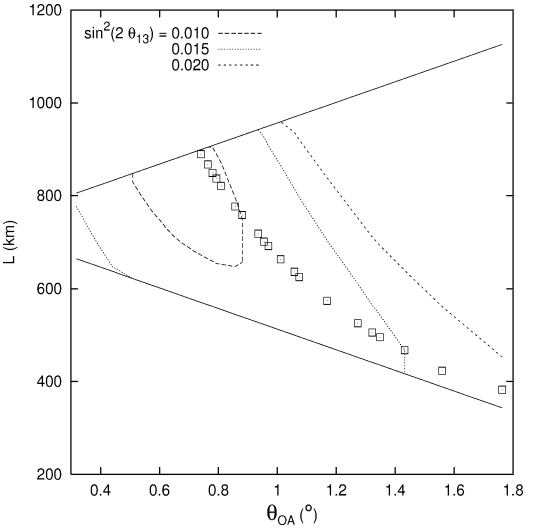

Fig. 4. Contours of $\sin^2 2\theta_{13}$ reach for distinguishing $\delta = 90°$ from the CP conserving values $\delta = 0°$ and $180°$ at 3σ (for the same $\mathrm{sgn}(\delta m^2_{31})$), plotted in the $(\theta_{\rm OA}, L_2)$ plane, when data from JHF and NuMI are combined. Other parameters and notation are the same as in Fig. 1. Results for $\delta = 270°$ are similar to those for $\delta = 90°$.

Fig. 4 shows contours of $\sin^2 2\theta_{13}$ reach for distinguishing $\delta = 90°$ from the CP conserving values $\delta = 0°$ and $180°$ at 3σ (with the same $\mathrm{sgn}(\delta m^2_{31})$), plotted in the $(\theta_{\rm OA}, L_2)$ plane, assuming ν and $\bar{\nu}$ data at both L_1 and L_2 are combined. The CP conserving solutions are sampled over a wide range in $\sin^2 2\theta_{13}$, not just for the same value of $\sin^2 2\theta_{13}$ as the $\delta m^2_{31} > 0$ solution. The CP reach in $\sin^2 2\theta_{13}$ can go as low as 0.01 for $\theta_{\rm OA} \simeq 0.5°$ to $0.9°$. Results for $\delta = 270°$ are similar to those for $\delta = 90°$.

Fig. 5 shows the minimum value of $\sin^2 2\theta_{13}$ for which δ can be distinguished from all CP conserving parameter sets with $\delta = 0°$ and $180°$, including those with the opposite $\mathrm{sgn}(\delta m^2_{31})$, at the 3σ level when $\theta_{\rm OA} = 0.74°$ and $L_2 = 890$ km, for several different values of δm^2_{21}. Fig. 5(a) shows the reaches if data from JHF and NuMI are combined, while Fig. 5(b) shows the reaches if data from NuMI only are used. For most values of δ, when δm^2_{21} is higher the CP effect is increased, and hence CP violation can be detected for smaller values of θ_{13}. However, there is a possibility that a CPV solution with one $\mathrm{sgn}(\delta m^2_{31})$ may not be as easily distinguishable from a CPC solution with the opposite $\mathrm{sgn}(\delta m^2_{31})$; this occurs, e.g., in Fig. 5(a) for $\delta m^2_{21} = 1 \times 10^{-4}$ eV^2, where the

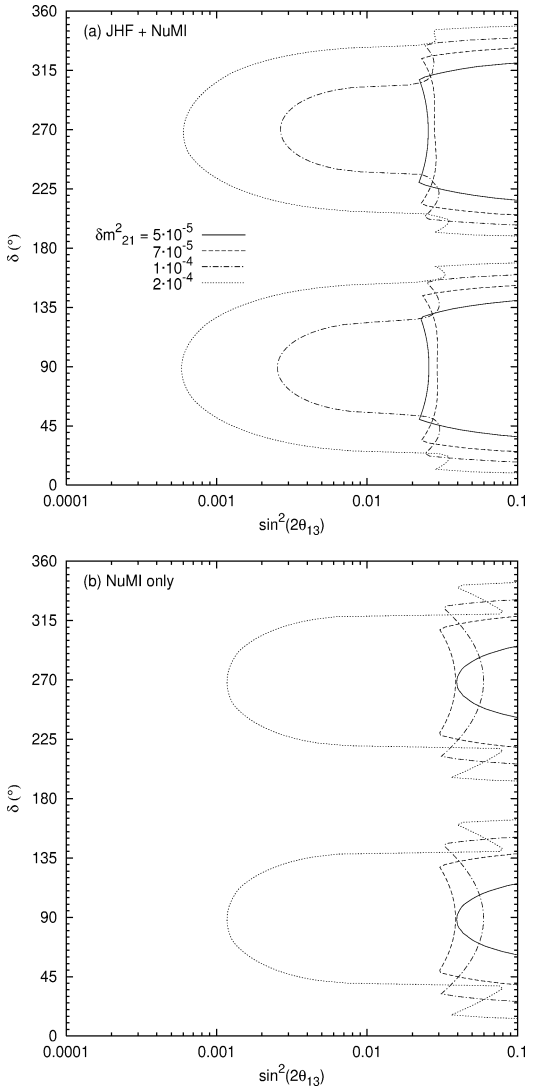

Fig. 5. Minimum value of $\sin^2 2\theta_{13}$ vs. CP phase δ for which δ can be distinguished from the CP conserving values $\delta = 0^\circ$ and 180° (with either sign of δm^2_{31}) at the 3σ level when (a) data from JHF and NuMI are combined, and (b) data from NuMI only are used. The baseline for JHF is $L_1 = 295$ km, while for NuMI $L_2 = 890$ km and $\theta_{\rm OA} = 0.74^\circ$. The curves are plotted for several values of the solar mass scale δm^2_{21} (in eV^2). Other parameters are the same as in Fig. 1.

predictions for ($\delta = 45^\circ$ and 135°, $\delta m^2_{31} > 0$) are close to those for ($\delta = 0^\circ$ and 180°, $\delta m^2_{31} < 0$), in this case the CP reach for those values of δ is about the same for $\delta m^2_{21} = 1 \times 10^{-4}$ eV^2 and $\delta m^2_{21} = 5 \times 10^{-5}$ eV^2.

We note that if data from only JHF are used (and assuming $\sin^2 2\theta_{13} \leqslant 0.1$) no value of the CP phase can be distinguished at 3σ from the CP conserving solutions when $\delta m^2_{21} \lesssim 8 \times 10^{-5}$ eV^2, principally because the intrinsic CP violation due to δ and the CP violation due to matter have similar magnitudes and it is hard to disentangle the two effects. For larger values of δm^2_{21}, the intrinsic CP effects are larger and CP violation can be established, e.g., if $\delta m^2_{21} = 1 \times 10^{-4}$ (2×10^{-4}) eV^2, maximal CP violation ($\delta = 90^\circ$ or 270°) can be distinguished from CP conservation at 3σ for $\sin^2 2\theta_{13} \gtrsim 0.006$ (0.001). Therefore, when $\delta m^2_{21} = 1 \times 10^{-4}$ eV^2, most of the CP sensitivity of the combined JHF plus NuMI data results from the JHF data, for $\delta m^2_{21} = 2 \times 10^{-4}$ eV^2 the two experiments contribute about equally to the CP sensitivity.

The boxes in Figs. 2 and 4 indicate the values of L_2 and $\theta_{\rm OA}$ for which the $\cos\delta$ terms in the average probabilities vanish for the second experiment. As indicated in the figures, these detector positions are good for both distinguishing sgn(δm^2_{31}) (see Fig. 2) and for establishing the existence of CP violation (see Fig. 4), especially for larger values of L_2. A good compromise occurs at $\theta_{\rm OA} \simeq 0.74^\circ$ with $L_2 \simeq 890$ km. In Ref. [15] it was shown that similar values for $\theta_{\rm OA}$ and L_2 using the NuMI off-axis beam gave a favorable figure-of-merit for the signal to background ratio; our analysis shows that such an off-axis angle and baseline is also very good for distinguishing sgn(δm^2_{31}) and establishing CP violation, when combined with superbeam data at $L_1 = 295$ km.

3.4. Resolving the $(\delta, \pi - \delta)$ ambiguity

If $L_2 \simeq 890$ km and $\theta_{\rm OA} \simeq 0.74^\circ$ are chosen for the location of the second experiment, as suggested in the previous section, then both the first and second experiments are effectively measuring $\sin\delta$, and it is impossible to resolve the $(\delta, \pi - \delta)$ ambiguity. Different values of L_2 and $\theta_{\rm OA}$ would be needed to distinguish δ from $\pi - \delta$.

Fig. 6 shows contours (in the space of possible L_2 and $\theta_{\rm OA}$) for the minimum value of $\sin^2 2\theta_{13}$ needed to distinguish $\delta = 0^\circ$ from $\delta = 180^\circ$ at the 2σ level using ν and $\bar\nu$ data from L_1 and L_2 (it is not possible to distinguish $\delta = 0^\circ$ from $\delta = 180^\circ$ at the 3σ level for any value of $\sin^2 2\theta_{13} \leqslant 0.1$). As with

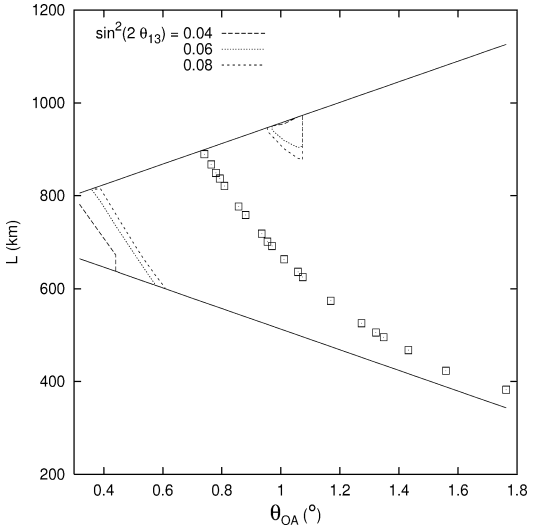

Fig. 6. Contours of $\sin^2 2\theta_{13}$ reach for distinguishing $\delta = 0°$ from $\delta = 180°$ (the $(\delta, \pi - \delta)$ ambiguity) at the 2σ level, plotted in the $(\theta_{\rm OA}, L_2)$ plane, when data from JHF and NuMI are combined. Other parameters and notation are the same as in Fig. 1.

Fig. 4, a wide range of $\sin^2 2\theta_{13}$ values are sampled for the alternate solutions. Two choices are possible: one with $\theta_{\rm OA} \lesssim 0.3°$–$0.5°$ and $L_2 \simeq 650$–775 km, and another near $\theta_{\rm OA} \simeq 1.0°$ with $L_2 \simeq 950$ km. The former choice does not do well in distinguishing $\mathrm{sgn}(\delta m^2_{31})$, while the latter choice is nearly optimal for $\mathrm{sgn}(\delta m^2_{31})$ sensitivity but significantly worse for CP violation sensitivity. Thus the ability to also resolve the $(\delta, \pi - \delta)$ ambiguity is rather poor, and comes at the expense of CPV sensitivity.

3.5. Resolving the $(\theta_{23}, \pi/2 - \theta_{23})$ ambiguity

If $\theta_{23} \neq \pi/4$, there is an additional ambiguity between θ_{23} and $\pi/2 - \theta_{23}$. This ambiguity gives two solutions for $\sin^2 2\theta_{13}$ whose ratio differs by a factor of approximately $\tan^2 \theta_{23}$, which can be as large as 2 if $\sin^2 2\theta_{23} = 0.9$ [11]. Assuming $L_1 = 295$ km for the first experiment, we could not find any experimental configuration of L_2 and $\theta_{\rm OA}$ for the second experiment that could resolve the $(\theta_{23}, \pi/2 - \theta_{23})$ ambiguity for $\sin^2 2\theta_{13} \leqslant 0.1$ at even the 1σ level for the entire range of detector sizes and source powers listed in Table 2. Therefore, we conclude that superbeams are not effective at resolving the $(\theta_{23}, \pi/2 - \theta_{23})$ ambiguity using ν_e and $\bar{\nu}_e$ appearance data. Since the approximate oscillation probability for $\nu_e \to \nu_\tau$ is given by the interchanges $\sin\theta_{23} \leftrightarrow \cos\theta_{23}$ and $\delta \to -\delta$ in the expression for the $\nu_\mu \to \nu_e$ probability, a neutrino factory combined with detectors having tau neutrino detection capability provides a means for resolving the $(\theta_{23}, \pi/2 - \theta_{23})$ ambiguity [11]. Another possibility is to measure survival of $\bar{\nu}_e$'s from a reactor, which to leading order is sensitive to $\sin^2 2\theta_{13}$ but not θ_{23} [34,35].

3.6. Dependence on other parameters

The foregoing analysis assumed $|\delta m^2_{31}| = 3 \times 10^{-3}$ eV^2. If the true value differs from this, then to sit on the peak (where the $\cos\delta$ terms vanish) requires tuning the beam energy and baseline according to the measured value of $|\delta m^2_{31}|$. JHF has the capability of varying the average E_ν from 0.4 to 1.0 GeV, which would correspond to realizing the peak condition for $|\delta m^2_{31}| = 1.6$–4.0×10^{-3} eV^2 [31]. In principle, NuMI can vary both L_2 and $\theta_{\rm OA}$ to be on the peak. If $|\delta m^2_{31}| < 3 \times 10^{-3}$ eV^2, then the best sensitivity to $\mathrm{sgn}(\delta m^2_{31})$ is obtained for larger $\theta_{\rm OA}$ and longer distances (the larger angle makes E_ν smaller while the longer distance enhances the matter effect), and the sensitivity is reduced (since the matter effect is smaller for smaller δm^2_{31}). The CP violation sensitivity is also reduced, although not as significantly. For larger values of $|\delta m^2_{31}|$ the sensitivity to $\mathrm{sgn}(\delta m^2_{31})$ is better, with CP violation sensitivity about the same.

The tuning of the experiments to the peak (where the $\cos\delta$ terms in the average probabilities vanish) requires knowledge of $|\delta m^2_{31}|$ before the experimental design is finalized. The values of $|\delta m^2_{31}|$ and θ_{23} will be well measured in the survival channel $\nu_\mu \to \nu_\mu$ measurements that would run somewhat before or concurrently with the appearance measurements being discussed here, but of course this information may not be available when the configurations for the off-axis experiments are chosen. If $|\delta m^2_{31}|$ is known to 10% at 3σ (the expected sensitivity of MINOS), then the sensitivities to $\mathrm{sgn}(\delta m^2_{31})$ and CP violation are not greatly affected by baselines that are slightly off-peak. If the baselines and neutrino energies for the superbeam experiments must be chosen before a 10% measurement of $|\delta m^2_{31}|$ can be made, a loss of sensitivity to $\mathrm{sgn}(\delta m^2_{31})$ could result by not being on

the peak. For example, if the experiments are designed for $|\delta m^2_{31}| = 3 \times 10^{-3}$ eV^2 but in fact $|\delta m^2_{31}| = 2.5 \times 10^{-3}$ eV^2, the 3σ sgn(δm^2_{31}) reach is less ($\sin^2 2\theta_{13} = 0.04$, compared to 0.03 for $|\delta m^2_{31}| = 3 \times 10^{-3}$ eV^2). If $|\delta m^2_{31}|$ is actually 2×10^{-3} eV^2, the 3σ sgn(δm^2_{31}) reach extends only down to $\sin^2 2\theta_{13} \simeq 0.075$, just a little below the CHOOZ bound.

Since the sgn(δm^2_{31}) determination has the worst reach in $\sin^2 2\theta_{13}$ (compared to the discovery reach and the CPV sensitivity), and since not knowing sgn(δm^2_{31}) can induce a CPV/CPC ambiguity, the measurement of sgn(δm^2_{31}) is crucial. If $|\delta m^2_{31}|$ is not known precisely, then the exact peak position is not known, and an off-axis angle and baseline should be chosen that will give a reasonable reach for sgn(δm^2_{31}) over as much of the allowed range of $|\delta m^2_{31}|$ as possible. For example, $\theta_{\rm OA} = 0.85°$–$0.90°$ and $L \simeq 930$ km gives a sgn(δm^2_{31}) reach that is fairly good for the range $|\delta m^2_{31}| = 2 \times 10^{-3}$ eV^2 to 4×10^{-3} eV^2. The reach for sgn(δm^2_{31}) is farthest from optimal at the extremes ($\sin^2 2\theta_{13} = 0.06$ vs. the best reach of 0.05 when $|\delta m^2_{31}| = 2 \times 10^{-3}$ eV^2 and 0.03 vs. the best reach of 0.02 when $|\delta m^2_{31}| = 4 \times 10^{-3}$ eV^2). But the CPV reach remains at least as good as the sgn(δm^2_{31}) reach for this range of $|\delta m^2_{31}|$.

The uncertainties in the parameters δm^2_{31}, $\sin^2 2\theta_{23}$, δm^2_{21}, and $\sin^2 2\theta_{12}$ will increase the region over which ambiguities can occur. As a test for this effect, we have used the approximate formulas for the probabilities to calculate the additional uncertainties in the event rates due to the expected uncertainties of these parameters and added them in quadrature to the statistical and systematic uncertainties. We assume 1σ errors of about 1% for the atmospheric parameters (which should be measured to very good precision in the survival channel of the JHF and NuMI experiments) and 5% for the solar parameters (which will be measured by a combination of solar and KamLAND data). When these additional uncertainties are included, we find that for the favorable case considered in Fig. 3 ($L = 890$ km and $\theta_{\rm OA} = 0.74°$ for the NuMI experiment) the reach in $\sin^2 2\theta_{13}$ for the determination of sgn(δm^2_{31}) is about the same for $\delta = 270°$ (where the $\delta m^2_{31} > 0$ and $\delta m^2_{31} < 0$ solutions do not overlap) and degraded by about 20–30% for $\delta = 90°$ (where the two solutions do overlap). However, there is also some information in the energy spectrum, even for the narrow spectrum of the off-axis beams, which would help to mitigate the effect of these uncertainties [16].

4. Summary

We summarize the important points of our Letter as follows:

(i) Two superbeam experiments at different baselines, each measuring $\nu_\mu \to \nu_e$ and $\bar\nu_\mu \to \bar\nu_e$ appearance, are significantly better at resolving the sgn(δm^2_{31}) ambiguity than one experiment alone. Using beams from a 4.0 MW JHF with a 22.5 kt detector 2° off axis at 295 km and a 1.6 MW NuMI with a 20 kt detector 0.7°–1.0° off axis at 875–950 km, sgn(δm^2_{31}) can be determined for $\sin^2 2\theta_{13} \gtrsim 0.03$ if $\delta m^2_{31} = 3 \times 10^{-3}$ eV^2. Sensitivities for other beam powers and detector sizes are given in Table 2.

(ii) For the most favorable cases, a higher value for the solar oscillation scale δm^2_{21} does not greatly change the sensitivity to sgn(δm^2_{31}) when ν and $\bar\nu$ data from two different baselines are combined (unlike the single baseline case, where the ability to determine sgn(δm^2_{31}) is significantly worse for $\delta m^2_{21} \gtrsim 5 \times 10^{-5}$ eV^2).

(iii) Running both experiments at the oscillation peaks, such that the $\cos\delta$ terms in the average probabilities vanish, provides good sensitivity to both sgn(δm^2_{31}) and to CP violation. On the other hand, the ability to resolve the $(\delta, \pi - \delta)$ ambiguity is lost, and the $(\theta_{23}, \pi/2 - \theta_{23})$ ambiguity is not resolved for any experimental arrangement considered. However, the $(\delta, \pi - \delta)$ and $(\theta_{23}, \pi/2 - \theta_{23})$ ambiguities do not substantially affect the ability to determine whether or not CP is violated (although the latter ambiguity could affect the inferred value of θ_{13} by as much as a factor of 2).

(iv) Since running at or near the oscillation peaks is favorable, knowledge of $|\delta m^2_{31}|$ to about 10% (from MINOS) before these experiments are run would be advantageous. If $|\delta m^2_{31}|$ is not known that precisely in advance, then the detector off-axis angle and baseline can still be chosen to give fairly good (though not optimal) sensitivities to sgn(δm^2_{31}) and CP violation.

We conclude that superbeam experiments at different baselines may greatly improve the prospects for determining the neutrino mass ordering in the three-neutrino model. Since a good compromise between determining $\mathrm{sgn}(\delta m^2_{31})$ and establishing the existence of CP violation is obtained when both experiments are tuned so that the $\cos\delta$ terms in the average probabilities approximately vanish, knowledge of $|\delta m^2_{31}|$ would be helpful for the optimal design for the experiments.

Acknowledgements

We thank A. Para for information on the NuMI off-axis beams, and A. Para and D. Harris for helpful discussions. This research was supported in part by the US Department of Energy under Grants Nos. DE-FG02-95ER40896, DE-FG02-01ER41155 and DE-FG02-91ER40676, and in part by the University of Wisconsin Research Committee with funds granted by the Wisconsin Alumni Research Foundation.

References

[1] T. Toshito, Super-Kamiokande Collaboration, hep-ex/0105023.
[2] J.N. Bahcall, M.H. Pinsonneault, S. Basu, Astrophys. J. 555 (2001) 990, astro-ph/0010346.
[3] Q.R. Ahmad, SNO Collaboration, nucl-ex/0204008;
Q.R. Ahmad, SNO Collaboration, nucl-ex/0204009.
[4] V. Barger, D. Marfatia, K. Whisnant, B.P. Wood, Phys. Lett. B 537 (2002) 179, hep-ph/0204253;
A. Bandyopadhyay, S. Choubey, S. Goswami, D.P. Roy, hep-ph/0204286;
J.N. Bahcall, M.C. Gonzalez-Garcia, C. Pena-Garay, hep-ph/0204314;
P. Aliani, V. Antonelli, R. Ferrari, M. Picariello, E. Torrente-Lujan, hep-ph/0205053;
P.C. de Holanda, A.Yu. Smirnov, hep-ph/0205241;
A. Strumia, C. Cattadori, N. Ferrari, F. Vissani, Phys. Lett. B 541 (2002) 327, hep-ph/0205261;
G.L. Fogli, E. Lisi, A. Marrone, D. Montanino, A. Palazzo, Phys. Rev. D 66 (2002) 053010, hep-ph/0206162;
M. Maltoni, T. Schwetz, M.A. Tortola, J.W. Valle, hep-ph/0207227.
[5] P. Alivisatos, et al., STANFORD-HEP-98-03.
[6] V. Barger, D. Marfatia, B.P. Wood, Phys. Lett. B 498 (2001) 53, hep-ph/0011251.
[7] MINOS Collaboration, Fermilab Report No. NuMI-L-375, 1998.
[8] A. Rubbia for the ICARUS Collaboration, Talk given at Skandinavian NeutrinO Workshop (SNOW), Uppsala, Sweden, February, 2001, which are available at http://pcnometh4.cern.ch/publicpdf.html.
[9] OPERA Collaboration, CERN/SPSC 2000-028, SPSC/P318, LNGS P25/2000, July, 2000.
[10] V. Barger, A.M. Gago, D. Marfatia, W.J. Teves, B.P. Wood, R.Z. Funchal, Phys. Rev. D 65 (2002) 053016, hep-ph/0110393.
[11] V. Barger, D. Marfatia, K. Whisnant, Phys. Rev. D 65 (2002) 073023, hep-ph/0112119.
[12] V. Barger, D. Marfatia, K. Whisnant, Phys. Rev. D 66 (2002) 053007, hep-ph/0206038.
[13] H. Minakata, H. Nunokawa, JHEP 0110 (2001) 001, hep-ph/0108085;
V.D. Barger, D. Marfatia, K. Whisnant, in: N. Graf (Ed.), Proc. of the APS/DPF/DPB Summer Study on the Future of Particle Physics, Snowmass, CO, 2001, hep-ph/0108090.
[14] T. Kajita, H. Minakata, H. Nunokawa, hep-ph/0112345.
[15] G. Barenboim, A. de Gouvea, M. Szleper, M. Velasco, hep-ph/0204208.
[16] P. Huber, M. Lindner, W. Winter, hep-ph/0204352.
[17] J. Burguet-Castell, M.B. Gavela, J.J. Gomez-Cadenas, P. Hernandez, O. Mena, Nucl. Phys. B 608 (2001) 301, hep-ph/0103258.
[18] M. Freund, P. Huber, M. Lindner, Nucl. Phys. B 615 (2001) 331, hep-ph/0105071;
J. Pinney, O. Yasuda, Phys. Rev. D 64 (2001) 093008, hep-ph/0105087;
A. Donini, D. Meloni, P. Magliozzi, hep-ph/0206034.
[19] J. Burguet-Castell, M.B. Gavela, J.J. Gomez-Cadenas, P. Hernandez, O. Mena, hep-ph/0207080.
[20] Y.F. Wang, K. Whisnant, J. Yang, B.L. Young, Phys. Rev. D 65 (2002) 073021, hep-ph/0111317;
K. Whisnant, J. Yang, B.L. Young, hep-ph/0208193.
[21] M. Aoki, K. Hagiwara, Y. Hayoto, T. Kobayashi, T. Nakaya, K. Nishikawa, N. Okamura, hep-ph/0112338.
[22] M. Apollonio, et al., CHOOZ Collaboration, Phys. Lett. B 466 (1999) 415, hep-ex/9907037.
[23] A. Cervera, et al., Nucl. Phys. B 579 (2000) 17, hep-ph/0002108;
A. Cervera, et al., Nucl. Phys. B 593 (2000) 731, Erratum.
[24] M. Freund, Phys. Rev. D 64 (2001) 053003, hep-ph/0103300.
[25] A. Dziewonski, D. Anderson, Phys. Earth Planet. Int. 25 (1981) 297.
[26] G.L. Fogli, E. Lisi, Phys. Rev. D 54 (1996) 3667, hep-ph/9604415.
[27] The expected JHF off-axis spectra with a 0.8 MW proton driver are available at http://neutrino.kek.jp/~kobayashi/50gev/beam/0101/.
[28] Anticipated neutrino spectra from a 0.4 MW NuMI for a range of off-axis angles can be found at http://www-numi.fnal.gov/fnal_minos/new_initiatives/beam/beam.html.
[29] D. Beavis, et al., E889 Collaboration, BNL preprint BNL-52459, April 1995.
[30] A. Para, M. Szleper, hep-ex/0110032.
[31] Y. Itow, et al., hep-ex/0106019.

[32] J. Hylen, et al., Conceptual design for the technical components of the neutrino beam for the main injector (NuMI), Fermilab-TM-2018, September 1997.
[33] W. Chou (Ed.), The proton driver study, Fermilab-TM-2136.
[34] G. Barenboim, A. de Gouvea, hep-ph/0209117.
[35] H. Minakata, H. Sugiyama, O. Yasuda, K. Inoue, F. Suekane, hep-ph/0211111.